

Nonlinear Transform Coding

Johannes Ballé, Philip A. Chou, David Minnen,
Saurabh Singh, Nick Johnston, Eirikur Agustsson,
Sung Jin Hwang, George Toderici

Google Research
Mountain View, CA 94043, USA

{jballe, philchou, dminnen, saurabhsingh,
nickj, eirikur, sjhwang, gtoderici}@google.com

Abstract

We review a class of methods that can be collected under the name nonlinear transform coding (NTC), which over the past few years have become competitive with the best linear transform codecs for images, and have superseded them in terms of rate–distortion performance under established perceptual quality metrics such as MS-SSIM. We assess the empirical rate–distortion performance of NTC with the help of simple example sources, for which the optimal performance of a vector quantizer is easier to estimate than with natural data sources. To this end, we introduce a novel variant of entropy-constrained vector quantization. We provide an analysis of various forms of stochastic optimization techniques for NTC models; review architectures of transforms based on artificial neural networks, as well as learned entropy models; and provide a direct comparison of a number of methods to parameterize the rate–distortion trade-off of nonlinear transforms, introducing a new one.

1 Introduction

There is no end in sight for the world’s reliance on multimedia communication. Digital devices have been increasingly permeating our daily lives, and with them comes the need to store, send, and receive images and audio ever more efficiently. Almost universally, transform coding (TC) has been the method of choice for compressing this type of data source.

In his 2001 article for IEEE Signal Processing Magazine (Goyal, 2001), Vivek Goyal attributed the success of TC to a divide-and-conquer paradigm: the practical benefit of TC is that it separates the task of decorrelat-

ing a source, from coding it. For comparison: in theory, any source can be optimally compressed using vector quantization (VQ) (Allen Gersho and Robert M. Gray, 1992). However, in general VQ quickly becomes computationally infeasible for sources of more than a handful of dimensions, mainly because the codebook of reproduction vectors as well as the search for the best reproduction of the source vector grow exponentially with the number of dimensions. TC simplifies quantization and coding by first mapping the source vector into a latent space via a decorrelating invertible transform, such as the Karhunen–Loève Transform (KLT), and then separately quantizing and coding each of the latent dimensions.

Much of the theory surrounding TC is based on an implicit or explicit assumption that the source is jointly

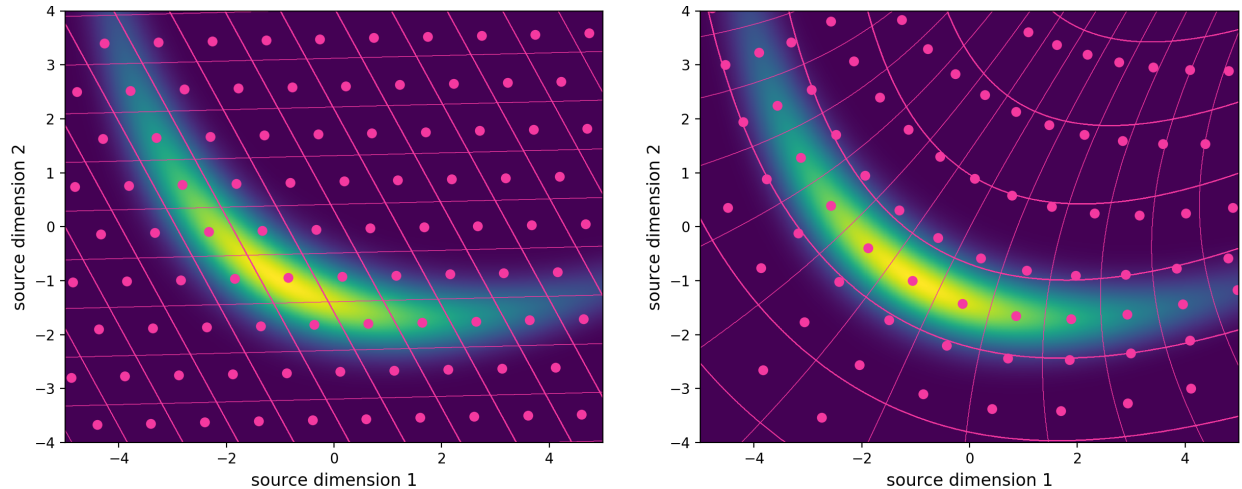


Figure 1: Linear transform code (left), and nonlinear transform code (right) of a banana-shaped source distribution, both obtained by empirically minimizing the rate–distortion Lagrangian (eq. (13)). Lines represent quantization bin boundaries, while dots indicate code vectors. While LTC is limited to lattice quantization, NTC can more closely adapt to the source, leading to better compression performance (RD results in fig. 3; details in section 3).

Gaussian, because this assumption allows for closed-form solutions. If the source is Gaussian, all that is needed to make the latent dimensions independent is decorrelation. When speaking of TC, it is almost always assumed that the transforms are linear, even if the source is far from Gaussian. In what follows, we focus on widening this perspective.

Until a few years ago, one of the fundamental constraints in designing transform codes was that determining nonlinear transforms that improve independence between latent dimensions is a difficult problem for high-dimensional sources, so in practice, not much research was conducted in directly using nonlinear transforms for compression. However, this premise has changed with the recent resurgence of artificial neural networks (ANNs). It is well-known that, with the right set of parameters, ANNs can approximate arbitrary functions (Leshno et al., 1993). It turns out that in combination with stochastic optimization methods, such as stochastic gradient descent (SGD), and massively parallel computational hardware, a nearly universal set of tools for approximating arbitrary functions has emerged, and these tools have also been

used in the context of image compression (Toderici, O’Malley, et al., 2016; Ballé, Laparra, and Simoncelli, 2017; Theis et al., 2017; Toderici, Vincent, et al., 2017; Rippel and Bourdev, 2017; Agustsson, Mentzer, et al., 2017). Even though these methods were developed from scratch, they have rapidly become competitive with modern conventional compression methods such as HEVC (HEVC 2013), which are the culmination of decades of incremental engineering efforts. This demonstrates, as it has in other fields, the flexibility and ease of prototyping that universal function approximation brings over designing methods manually, and the power of developing methods in a data-driven fashion.

This paper reviews some of the recent developments in data-driven lossy compression; in particular, we focus on a class of methods that can be collectively called *nonlinear transform coding* (NTC), providing insights into its capabilities and challenges. We assess the empirical rate–distortion (RD) performance of NTC with the help of simple example sources: the Laplace source and a two-dimensional banana-shaped distribution. To this end, we introduce a novel variant of entropy-constrained vector quantization (ECVQ) algo-

rithm (Chou, Lookabaugh, and Robert M Gray, 1989). Further, we provide insights into various forms of optimization techniques for NTC models and review ANN-based transform architectures, as well as entropy modeling for NTC. A further contribution of this paper is to provide a direct comparison of a number of methods to parameterize the RD trade-off, and to introduce a new one.

In the next section, we first review stochastic gradient optimization of the RD Lagrangian, a necessary tool for optimizing ANNs for lossy compression. We introduce variational ECVQ, illustrating this type of optimization. VECVQ also serves as a baseline to evaluate nonlinear transform coding (NTC) in the subsequent section. In that section, we discuss various approaches for approximating the gradient of the NTC objective and review ANN architectures. Section 4 reviews entropy modeling via learned forward and backward adaptation, and illustrates their performance gains on image compression. Section 5 compares several ways of parameterizing the transforms to achieve multiple points along the RD curve with a single set of transforms, without significantly losing performance. The last section discusses connections to related work and concludes the paper.

2 Stochastic rate–distortion optimization

Consider the following lossy compression scenario. Alice is drawing vectors $\mathbf{x} \in \mathbb{R}^N$ from some data source, whose probability density function we denote p_{source} . Here, Alice is concerned with compressing each vector into a bit sequence, communicating this sequence to Bob, who then uses the information to reconstruct an approximation to \mathbf{x} . Each possible vector \mathbf{x} is approximated using a codevector $\mathbf{c}_k \in C$, where $C = \{\mathbf{c}_k \in \mathbb{R}^N \mid 0 \leq k < K\}$ is called the codebook. Once the codevector index $k = e(\mathbf{x})$ for a given \mathbf{x} is determined using the encoder $e(\cdot)$, Alice subjects it to lossless entropy coding, such as Huffman coding or arithmetic coding, which yields the bit sequence of nominal length $s(k)$. In what follows, we'll assume that the performance of this entropy coding method is optimized to closely approximate the theoretical limit, i.e., that Alice and Bob

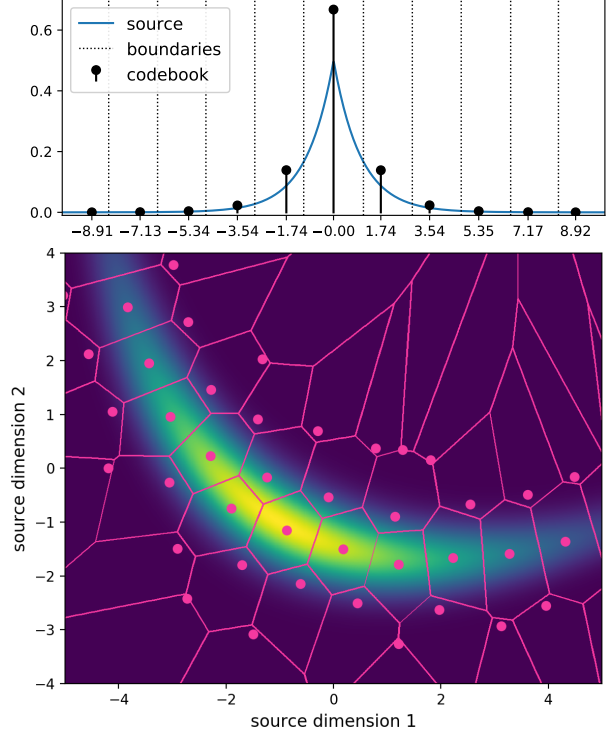


Figure 2: Top: A near-optimal entropy-constrained scalar quantizer of a standard Laplacian source, found using the VECVQ algorithm (eq. (5)). Bottom: an entropy-constrained vector quantizer of a banana-shaped source, found using the same algorithm.

share an estimate of the marginal probability distribution of k , also called an entropy model, $P(k)$, and that $s(k) \approx -\log_2 P(k)$. To the extent that $P(k)$ approximates $M(k) = \mathbb{E}_{\mathbf{x} \sim p_{\text{source}}} \delta(k, e(\mathbf{x}))$, the true marginal distribution of k (where δ denotes the Kronecker delta function), $s(k)$ is close to optimal, since codes of length $-\log_2 M(k)$ would achieve the lowest possible average rate, the entropy of k . Since Alice and Bob also share knowledge of the codebook, Bob can decode the index k and finally look up the reconstructed vector \mathbf{c}_k .

To optimize the efficiency of this scheme, Alice and Bob seek to simultaneously minimize the cross entropy of the index under the entropy model (the rate) as well as the distortion between \mathbf{x} and the reconstructed vec-

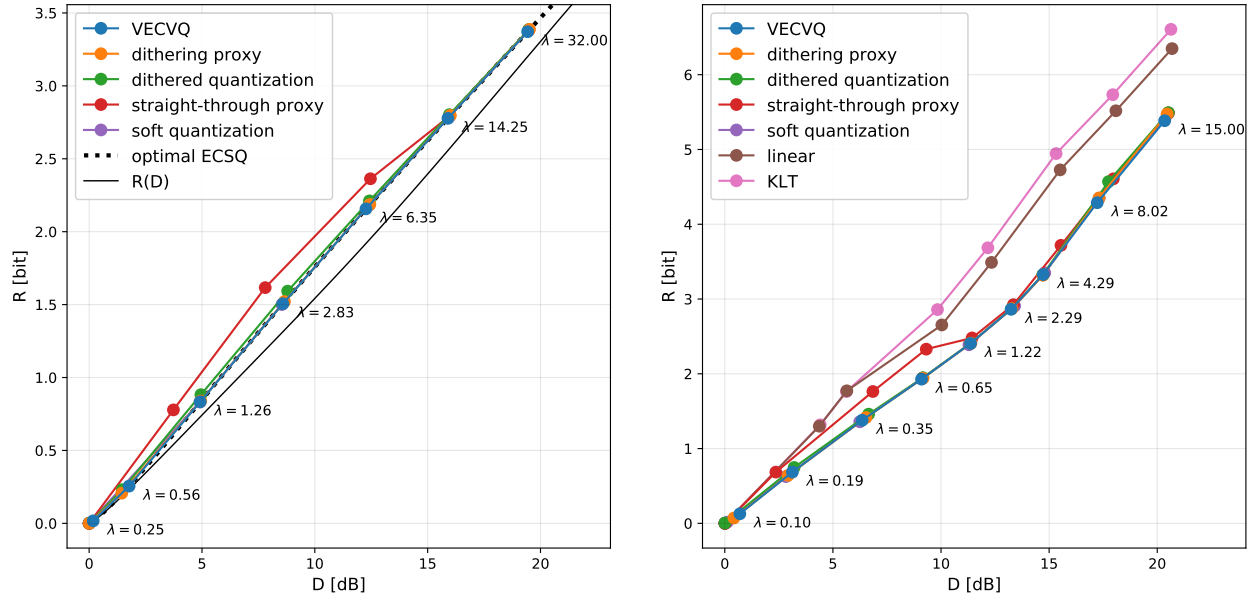


Figure 3: Left: rate-distortion performance of different quantizers for standard Laplace source. Both VECVQ and NTC with optimized offset ("dithering proxy") recover the optimal entropy-constrained scalar quantizer established by Sullivan (1996). NTC with randomized offset ("dithered quantization") is slightly suboptimal at lower rates, as predicted by theory. The NTC trained with the straight-through proxy is unstable at low rates. Using the dithering proxy with explicit soft quantization recovers the optimal quantizer as well. $R(D)$ indicates the information-theoretic rate-distortion function, $R(D) = \inf_{p(\hat{x}|x)} \{I(x; \hat{x}) \text{ s.t. } \mathbb{E}[d(x, \hat{x})] \leq D\}$ (achievable only in the limit of large block sizes, not with a scalar quantizer). Right: rate-distortion performance of different quantizers for banana source. NTC closely matches the performance of VECVQ; the straight-through variant diverges at low rates. The linear TC trained for the same objective performs significantly worse. Constraining it to the KLT is not necessarily optimal, as pointed out by Goyal (2001).

tor, quantified by some distortion measure d :

$$L = \mathbb{E}_{\mathbf{x} \sim p_{\text{source}}} [-\log_2 P(k) + \lambda d(\mathbf{x}, \mathbf{c}_k)], \quad (1)$$

with $k = e(\mathbf{x})$ is determined by the algorithm $e(\cdot)$ that chooses a codebook index for each possible source vector. Many authors have formulated this as a minimization problem over one of the quantities given a hard constraint on the other (Cover and Thomas, 2006). In this paper, we consider the Lagrangian relaxation of the distortion-constrained problem, with the Lagrange multiplier λ on the distortion term determining the trade-off between rate and distortion.

The top panel of fig. 2 illustrates a lossy compression method for a simple, one-dimensional Laplacian source, optimized for squared error distortion (i.e., $d(\mathbf{x}, \hat{\mathbf{x}}) = \|\mathbf{x} - \hat{\mathbf{x}}\|_2^2$). The source distribution is plotted in blue. The codebook vectors are represented by the horizontal locations of the black stalks, while the height of each stalk is proportional to the likelihood of that code vector under the entropy model P . Dotted lines delineate the quantization bins, i.e., the intervals for which all source values get mapped to a given codebook value (the one within the respective interval). For Laplacian sources, the minimizer of L has been studied by Sullivan (1996). It is characterized by equal-width quantization bins and equidistant code vectors, except for the center bin (coinciding with the mode of the source distribution); both characteristic features are present in the figure up to small deviations. The bottom panel of the same figure visualizes a vector quantizer for a banana-shaped source distribution. The boundaries between quantization bins are shown as pink lines, while the code vectors are rendered as discs. Note the presence of hexagon-like bins, which are a feature of optimal VQ for squared-error distortions.

2.1 Variational entropy-constrained vector quantization

To generate both of the results in fig. 2, we used a novel algorithm for entropy-constrained vector quantization based on directly minimizing eq. (1). To begin, without loss of generality, we parameterize the entropy model as

$$P(k) = \frac{\exp(a_k)}{\sum_{j=0}^{K-1} \exp(a_j)}. \quad (2)$$

Then, denoting model parameters $\Theta = \{a_k, \mathbf{c}_k \mid 0 \leq k < K\}$, we define the sample loss

$$\ell_{\Theta}(k, \mathbf{x}) = -\log_2 P(k) + \lambda d(\mathbf{x}, \mathbf{c}_k) \quad (3)$$

and the encoder function

$$e_{\Theta}(\mathbf{x}) = \arg \min_k \ell_{\Theta}(k, \mathbf{x}), \quad (4)$$

where we have made explicit their dependence on the parameters Θ . We express eq. (1) as

$$L_{\text{VQ}} = \mathbb{E}_{\mathbf{x}} \ell_{\Theta}(e_{\Theta}(\mathbf{x}), \mathbf{x}) = \mathbb{E}_{\mathbf{x}} \min_k \ell_{\Theta}(k, \mathbf{x}), \quad (5)$$

which we now wish to minimize over Θ using stochastic gradient descent (SGD). SGD relies on a Monte Carlo approximation of the expectation, and the fact that expectations and derivatives are both linear operators, whose order can be exchanged using the dominated convergence theorem. Thus

$$\frac{\partial}{\partial \Theta} L_{\text{VQ}} = \mathbb{E}_{\mathbf{x}} \frac{\partial}{\partial \Theta} \min_k \ell_{\Theta}(k, \mathbf{x}), \quad (6)$$

which can be approximated by the sample expectation

$$\frac{\partial}{\partial \Theta} L_{\text{VQ}} \approx \frac{1}{B} \sum_{\{\mathbf{x}_b \sim p_{\text{source}} \mid 0 \leq b < B\}} \frac{\partial \ell_{\Theta}(k_b, \mathbf{x}_b)}{\partial \Theta}, \quad (7)$$

with $k_b = e_{\Theta}(\mathbf{x}_b)$. This Monte Carlo approximation is an unbiased estimator of the derivative of L_{VQ} based on averaging the derivatives of ℓ over a batch of B source vector samples.

Minimization of L_{VQ} will fit the entropy model to the marginal distribution of k , $M(k) = \mathbb{E}_{\mathbf{x} \sim p_{\text{source}}} \delta(k, e(\mathbf{x}))$, as well as adjust the codebook vectors to minimize distortion. To see this, add and subtract the expected negative log likelihood of k under the marginal to eq. (5):

$$L_{\text{VQ}} = D_{\text{KL}}[M \parallel P] + \mathbb{E}_{\mathbf{x}} [-\log_2 M(k) + \lambda d(\mathbf{x}, \mathbf{c}_k)]. \quad (8)$$

Since only the first term depends on the parameters of P , minimizing L_{VQ} results in fitting P to M by minimizing their Kullback–Leibler (KL) divergence. Additionally, each \mathbf{c}_k is adjusted to minimize the distortion between it and all source vectors getting mapped to k , since only the second term depends on the codebook. Also note that since the KL divergence is non-negative, L_{VQ} can be interpreted as an upper bound

on the second term, which is the rate–distortion objective for the optimal choice of entropy model. This can be likened to variational Bayesian inference, in which a *variational* approximation (P) to an unobserved true distribution (M) is found by minimizing an upper bound on the true objective. We therefore name this method variational entropy-constrained vector quantization (VECVQ).¹ Note that, since P as defined in eq. (2) can represent arbitrary distributions, the variational approximation here is capable of recovering the true marginal, i.e., the Kullback–Leibler divergence can converge to zero.

In the left panel of fig. 3, we plot the operational rate–distortion function of the optimal entropy-constrained scalar quantizer due to Sullivan (1996) as well as the empirical rate–distortion function for the VECVQ algorithm for the same Laplace source. The plot shows that the algorithm recovers the theoretical optimum. Since it is constrained only by the size of the codebook, we can use the algorithm as an empirical lower bound on the rate–distortion objective of more constrained compression methods, such as nonlinear transform coding, even for source distributions for which no theoretical optimum is presently known. As an example, consider the more complex banana distribution in the right panel: the nonlinear transform coders trained with the dithering proxy (to be discussed in the next section) perform ever so slightly worse than VECVQ.

3 Nonlinear transform coding

It is easy to modify eq. (1) to accommodate *nonlinear* transform coding. Rather than explicitly enumerating the codebook vectors, we consider mapping the source vectors into a latent space \mathbb{R}^M and back via a pair of transforms. Quantization and compression takes place in the latent space. Specifically, we define the analysis

¹The VECVQ algorithm inherits from two methods. The first is the ECVQ algorithm of Berger (1972), Favardin and Modestino (1984), and Chou, Lookabaugh, and Robert M Gray (1989), which minimizes eq. (1) using a clustering algorithm instead of gradient descent. The second is the online K -means algorithm of Bottou and Bengio (1995), which minimizes the distortion part of eq. (1), $\mathbb{E}_x[d(x, c_k)]$, using gradient descent. Both ECVQ and the online K -means algorithms derive in turn from the generalized Lloyd algorithm (Lloyd, 1982; Max, 1960; MacQueen et al., 1967; Linde, Buzo, and R. M. Gray, 1980).

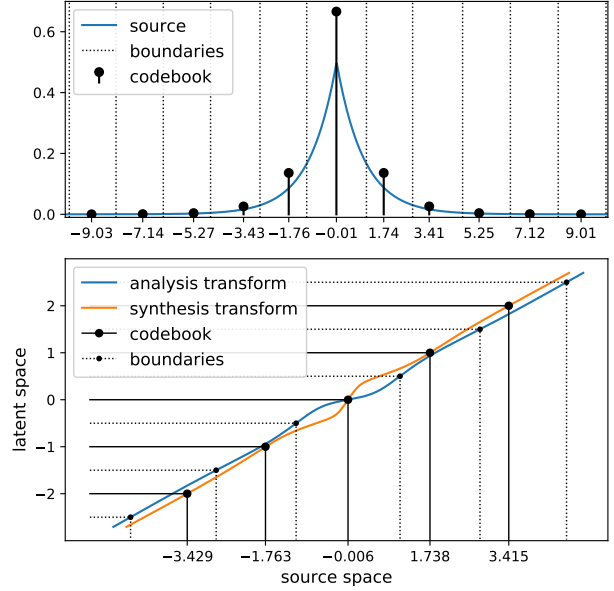


Figure 4: A near-optimal nonlinear transform code of a standard Laplacian source, obtained by minimizing the dithering rate–distortion proxy (eq. (13)).

transform as a parametric function $y = g_a(x)$, implemented by a neural network with parameters ϕ , and the synthesis transform as a function $c = g_s(y)$, with parameters θ . We can write the rate–distortion objective as:

$$L_{\text{NTC}} = \mathbb{E}_x \left[-\log_2 P(\lfloor g_a(x) \rfloor) + \lambda d(x, g_s(\lfloor g_a(x) \rfloor)) \right], \quad (9)$$

where $\lfloor \cdot \rfloor$ denotes uniform quantization (rounding to integers). P is now a probability distribution over a space of integer vectors, which take the role of the codebook index k in eq. (1).

As an example, consider the nonlinear transform coder illustrated in fig. 4. Again, we plot the effective codebook vectors and quantization boundaries on top of the source distribution. However, unlike the example in fig. 2, this quantization scheme is defined indirectly via the analysis and synthesis transforms, as illustrated in the bottom panel of fig. 4. The analysis transform maps the space of source values to the latent

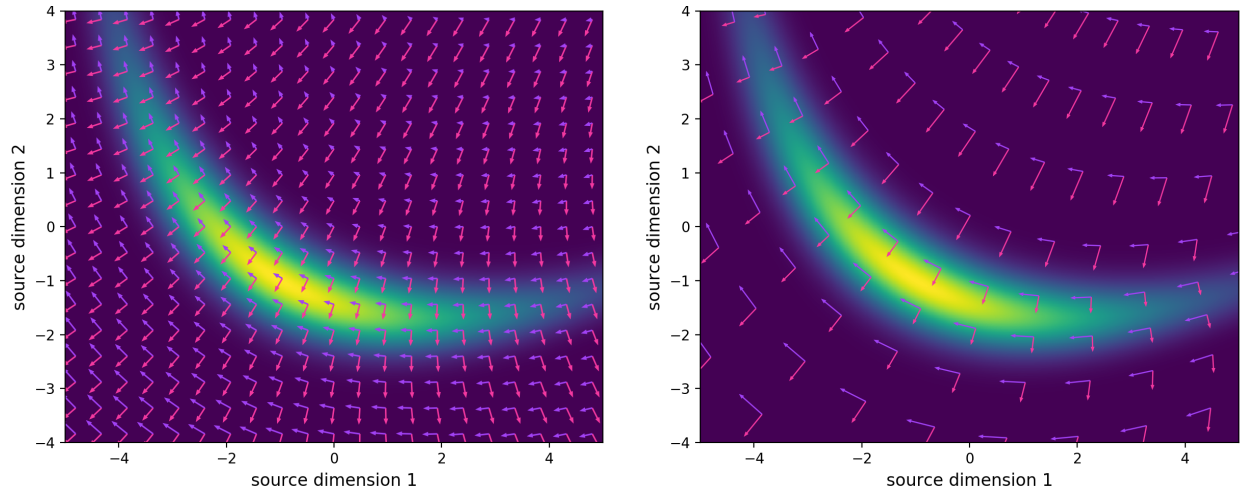


Figure 5: Location-dependent Jacobian matrices $\partial g_a(x)/\partial x$ (left; arrows visualize local Jacobian inverse) and $\partial g_s(y)/\partial y$ (right; arrows visualize local Jacobian) of a model optimized for squared error distortion on the banana source. The transforms form a local orthogonalization of the source density.

space (blue curve). In this space, uniform quantization is applied, rounding values between half-integers to full integers. These integer values are then mapped back into the source space using the synthesis transform (orange curve).

There are a few key observations here: First, the analysis transform determines the effective quantization bins. In particular, its intersections with the dotted lines, corresponding to half-integers in the latent space, give rise to quantization bins of varying size in the source space. Second, the synthesis transform determines the effective codebook vectors. Notably, the full behavior of the synthesis transform as determined by the optimization procedure does not matter – only its values at integer locations are relevant. Third, since the transforms are not constrained to be exact inverses of each other, using uniform quantization in the latent space is sufficient to enable codebook vectors to be located anywhere in the corresponding quantization bins (technically, even outside of it). Nonlinear transform coding thus generalizes companding (Bennett, 1948; A. Gersho, 1979), which permits implementing non-uniform quantization using uniform quantizers; with nonlinear transforms, the quantization step size can be fixed to one without loss of generality (parameterizing

the model for different rate–distortion trade-offs is discussed in section 5).

Figure 1 illustrates linear and non-linear transform coding of the banana distribution shown in fig. 2. Both the linear and nonlinear transform codes are designed to minimize eq. (9) under their respective constraints. Because the linear transform coder is constrained to affine transformations, the method effectively amounts to a lattice quantizer in the source space (left panel). Note that the linear transform is not orthogonal and hence is *not* the KLT, as would be optimal if the source distribution were Gaussian.

The non-linear transform coder has more flexibility, and can adapt the shapes of its quantization bins to better fit the source distribution (right panel). Note that in both cases, since invertibility of the transforms is not enforced, codebook vectors do not necessarily appear in consistent locations relative to their bins. Their optimal locations, for squared error distortions, are at the conditional mean of their respective cells. Both coders reflect this by shifting the codebook vectors closer to the high-probability regions of the source distribution. This may come at the expense of reconstruction accuracy in low-probability regions – in the nonlinear example, some low-probability codebook vectors even lie

outside of their respective bins – because the behavior of the method in these regions often does not contribute much to the overall objective. Another reason for this trade-off may be limitations in the parameterizations of the transforms. This is further examined in section 3.2.

Although the optimized nonlinear analysis and synthesis transforms shown in fig. 1 (right) are globally non-linear, they are of course differentiable, and hence can be viewed as locally linear. In regions of the data distribution contributing sufficiently to the training objective, they locally resemble KLTs in that they are approximately orthogonalized (fig. 5). Specifically, at each point x , the columns of the matrix $[G_a(x)]^{-1}$, which is the inverse of the Jacobian matrix $G_a(x) = \partial g_a(x)/\partial x$ of the analysis transform, are approximately orthogonal to each other, as shown in the quiver plot of the left panel of the figure, for points x selected on a regular grid. Thus, the columns of $G_a(x)$ are also approximately orthogonal to each other. Likewise, the columns of the Jacobian matrix $G_s(y) = \partial g_s(y)/\partial y$ of the synthesis transform are approximately orthogonal to each other, as shown in the quiver plot of the right panel, for points $\tilde{x} = g_s(y)$ where points y are selected on a regular grid. For points x in the neighborhood of x_0 , $(y - y_0) \approx G_a(x_0)(x - x_0)$ is approximately a scaled orthonormal analysis transform, and $(\tilde{x} - \tilde{x}_0) \approx G_s(y_0)(y - y_0)$ is approximately its inverse, where $y_0 = g_a(x_0)$ and $\tilde{x}_0 = g_s(y_0)$.

While more can be said about the local properties of the analysis and synthesis transforms, for now, let us consider the transforms as “black boxes” that simply serve to approximate the optimal transforms.

3.1 Optimization and proxy rate-distortion loss

Note that in the VECVQ loss given in eq. (5), the encoder function is defined by exhaustively minimizing over all possible codes. As such, it can be folded into a minimum over the sample loss ℓ , which is differentiable with respect to almost all x . If we were to choose another encoder function with trainable parameters of its own, we would not be able to obtain a gradient of the loss function with respect to them that is useful for SGD. The gradient would be zero for almost all x , be-

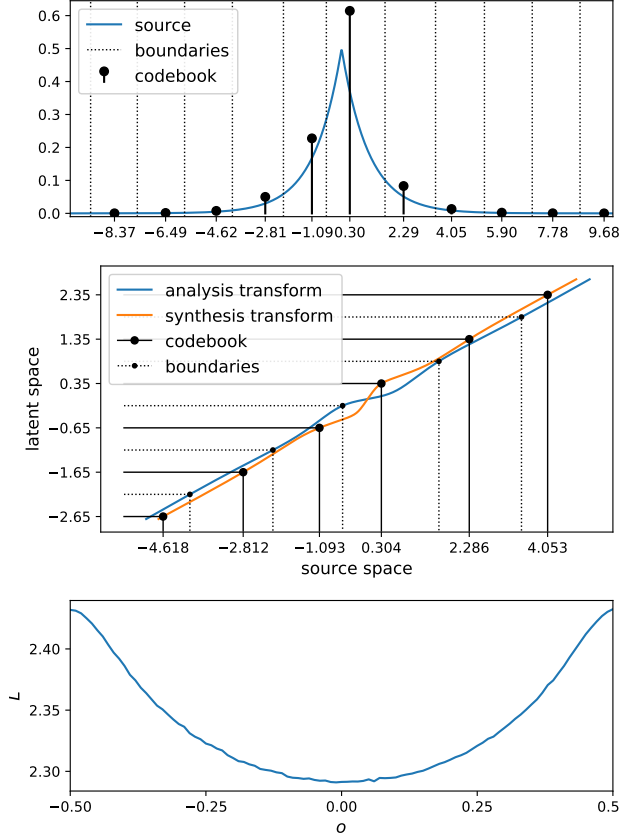


Figure 6: The same instance of NTC as in fig. 4, obtained by minimizing $\mathbb{E}_o L_{\text{NTC},o}$. For this figure, a sub-optimal offset was chosen post hoc. Top: visualization of effective quantizer. Center: analysis and synthesis transforms giving rise to the quantizer. Note that the transforms themselves are identical to the ones in fig. 4, but the quantization in the latent space is performed with an offset $o = .35$. Bottom: $L_{\text{NTC},o}$ as a function of o .

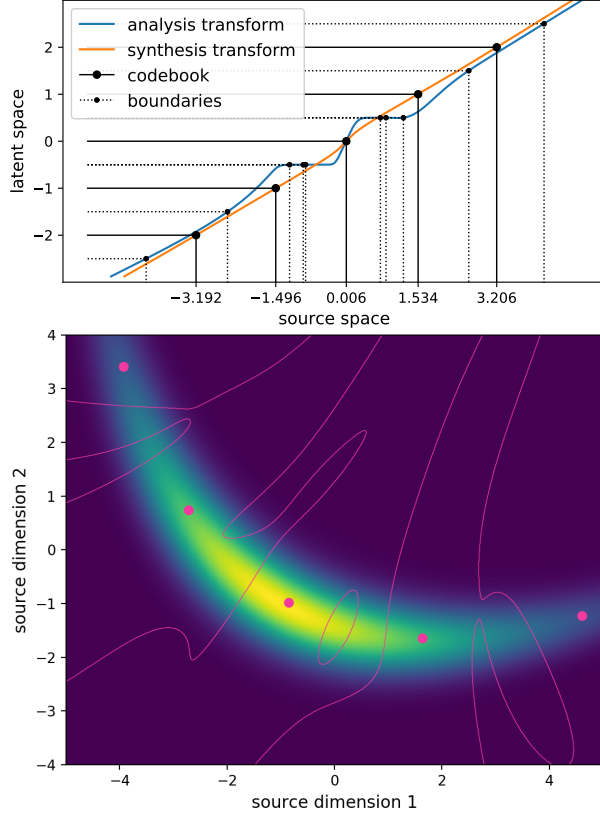


Figure 7: Instabilities observed with straight-through proxy objective at low rates for the Laplace (top) and banana (bottom) distribution. While the synthesis transform tends to be smoother, the analysis transform begins oscillating around the locations of bin boundaries, leading effectively to discontinuous quantization bins.

cause e is integer valued. This problem also applies to eq. (9) due to the quantizer. Derivatives of the loss with respect to any parameter of the analysis transform are zero almost everywhere. However, when employing dithered quantization (i.e., randomizing the quantization offset) (Schuchman, 1964), this problem can be avoided (Ballé, Laparra, and Simoncelli, 2016b).

Consider uniformly sampling one random quantization offset per latent dimension $\mathbf{o} \in [-\frac{1}{2}, \frac{1}{2}]^M$, and formulating the following loss function as an expectation over it:

$$\mathbb{E}_{\mathbf{o}} L_{\text{NTC}, \mathbf{o}} = \mathbb{E}_{\mathbf{x}, \mathbf{o}} \left[-\log_2 P(\lfloor g_a(\mathbf{x}) - \mathbf{o} \rfloor; \mathbf{o}) + \lambda d(\mathbf{x}, g_s(\lfloor g_a(\mathbf{x}) - \mathbf{o} \rfloor + \mathbf{o})) \right], \quad (10)$$

where $L_{\text{NTC}, \mathbf{o}}$ is the loss for a given offset \mathbf{o} , and $P(\cdot; \mathbf{o})$ is an entropy model conditioned on \mathbf{o} . (Note that all else being equal, the marginal distribution of the quantized latents changes with the offset.) This loss function is still not differentiable with respect to the parameters of g_a . However, it can be shown that it has a differentiable equivalent. Let us consider both terms separately. For the rate term, we have

$$\begin{aligned} & -\mathbb{E}_{\mathbf{x}, \mathbf{o}} \log_2 P(\lfloor g_a(\mathbf{x}) - \mathbf{o} \rfloor; \mathbf{o}) \\ &= -\mathbb{E}_{\mathbf{x}, \mathbf{o}} \sum_{\mathbf{k} \in \mathbb{Z}^M} \delta(\lfloor g_a(\mathbf{x}) - \mathbf{o} \rfloor = \mathbf{k}) \log_2 P(\mathbf{k}; \mathbf{o}) \\ &= -\mathbb{E}_{\mathbf{x}} \int \cdots \int_{-\frac{1}{2}}^{\frac{1}{2}} d\mathbf{o} \sum_{\mathbf{k} \in \mathbb{Z}^M} \delta(\|g_a(\mathbf{x}) - \mathbf{o} - \mathbf{k}\|_{\infty} \leq \frac{1}{2}) \log_2 P(\mathbf{k}; \mathbf{o}) \\ &= -\mathbb{E}_{\mathbf{x}} \int \cdots \int_{-\infty}^{\infty} d\mathbf{v} \delta(\|g_a(\mathbf{x}) - \mathbf{v}\|_{\infty} \leq \frac{1}{2}) \log_2 p(\mathbf{v}) \\ &= -\mathbb{E}_{\mathbf{x}} \int \cdots \int_{-\frac{1}{2}}^{\frac{1}{2}} d\mathbf{u} \log_2 p(g_a(\mathbf{x}) + \mathbf{u}) \\ &= -\mathbb{E}_{\mathbf{x}, \mathbf{u}} \log_2 p(g_a(\mathbf{x}) + \mathbf{u}), \end{aligned} \quad (11)$$

where δ is the Kronecker delta function, we define $\mathbf{v} = \mathbf{k} + \mathbf{o}$ and $p(\mathbf{v}) = P(\lfloor \mathbf{v} \rfloor; \mathbf{v} - \lfloor \mathbf{v} \rfloor)$, and consider $\mathbf{u} \in [-\frac{1}{2}, \frac{1}{2}]^M$ uniformly distributed. It is easy to show that p is non-negative and integrates to one, and hence represents a probability density function. We can thus interpret p as a continuous equivalent of an entropy

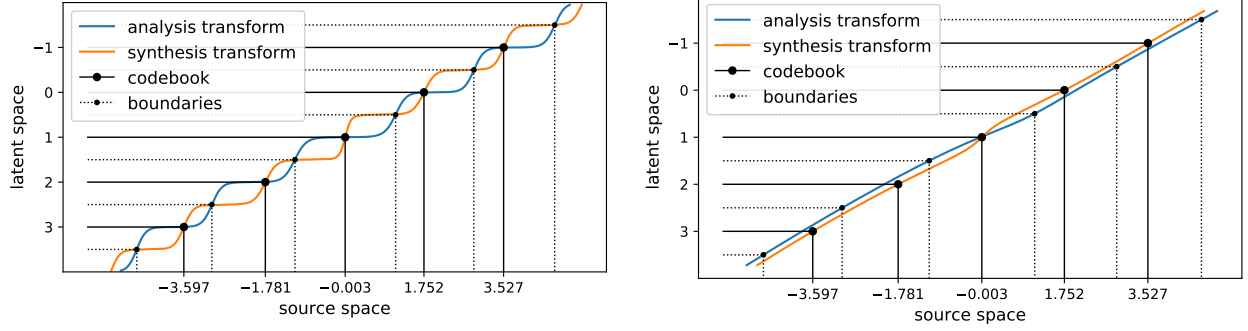


Figure 8: Transforms for Laplace source with explicit soft quantization due to Agustsson and Theis (2020). Left: ANN transforms including the explicit soft quantization. Right: ANN transforms excluding the explicit soft quantization. With this technique, the ANNs themselves can implement smoother (i.e., in some sense, simpler) functions.

model for the “noisy” latents $g_a(x) + u$. For the distortion term, we have

$$\mathbb{E}_{x,o} d(x, g_s(\lfloor g_a(x) - o \rfloor + o)) = \mathbb{E}_{x,u} d(x, g_s(g_a(x) + u)), \quad (12)$$

since dithered quantization and additive uniform noise have the same marginal distribution (i.e., integrating out o and u is equivalent). For a proof, refer to Schuchman (1964).

Hence, we can now write

$$\mathbb{E}_o L_{\text{NTC},o} = \mathbb{E}_{x,u} \left[-\log_2 p(g_a(x) + u) + \lambda d(x, g_s(g_a(x) + u)) \right], \quad (13)$$

which is differentiable with respect to parameters of g_a (as well as g_s and p , if we assume the latter to be some parametric density model), and which can be minimized via SGD analogously to eq. (7).

Note that as in eq. (8), we can interpret eq. (13) as a variational upper bound on the true marginal:

$$\mathbb{E}_o L_{\text{NTC},o} = D_{\text{KL}}[m \parallel p] + \mathbb{E}_{x,u} \left[-\log_2 m(g_a(x) + u) + \lambda d(x, g_s(g_a(x) + u)) \right], \quad (14)$$

where $m(v) = \mathbb{E}_{x,u} \delta(v, g_a(x) + u)$ is the marginal

distribution of the noisy latents.² As such, minimizing eq. (13) results in fitting the continuous entropy model p to the marginal. Note that, unlike in the case of VECVQ, the KL divergence may not converge to zero, as for high-dimensional source distributions such as images, the entropy model will generally not be capable of representing the marginal accurately. Section 4 talks about this in more detail.

There is one caveat with using dithered quantization for compression itself: this is not necessarily optimal, since $\mathbb{E}_o L_{\text{NTC},o} \geq \min_o L_{\text{NTC},o}$ (fig. 3, left panel, illustrates this). If we do not wish to use dithered quantization, we can still use eq. (13) as a proxy loss for transform coding with a quantization offset known to both Alice and Bob. Note that it optimizes the parameters of the model to do well on average. This suggests a simple algorithm for stochastic optimization of a transform coder:

1. Minimize eq. (13).
2. Determine which offsets o minimize $L_{\text{NTC},o}$. If the continuous entropy model p is accurate enough, this can be done without re-estimating the discrete entropy models, since $P(k; o) = p(k + o)$.

²This formally establishes an equivalence between rate-distortion optimized nonlinear transform coding and variational Bayes, specifically β -variational autoencoders (Ballé, Laparra, and Simoncelli, 2017; Higgins et al., 2017; Alemi et al., 2018).

A suboptimal choice of offset for an NTC encoding a Laplace source is illustrated in fig. 6, along with a plot of $L_{\text{NTC},o}$ as a function of o for the same source. Note that optimizing the dithering proxy loss leads to the transforms becoming increasingly curved around the central quantization bin, to accommodate arbitrary choices of o . Because the analysis transform becomes increasingly flat around the center, and the synthesis transform increasingly steep, the effective code vector and quantization bin around the mode of the distribution is skewed towards the near-optimal quantizer illustrated in fig. 4. It could be argued that, to minimize the loss function, this should happen in all bins. However, we haven't observed this empirically, presumably due to ANNs naturally favoring smoother functions, and the other bins not contributing enough to the value of the loss function.

While Ballé, Laparra, and Simoncelli (2017) explicitly perform a grid search over o , some follow-up papers have resorted to a simple heuristic: guided by the result that for Laplacian distributions, it is optimal to pick an offset that aligns the mode of the source distribution with a codebook vector, one can simply pick an offset for each latent dimension such that one of the quantization bins is centered on the mode (or, in case that is computationally intractable, the median) of the entropy model p (Ballé, Minnen, Singh, et al., 2018; Minnen, Ballé, and Toderici, 2018). Other authors choose to retain the dithering proxy for the rate term, but use a *straight-through* gradient estimate for the distortion term (effectively computing the distortion loss with constant-offset quantization during training, but replacing the gradient expression of the quantization operation with the identity function (Agustsson, Minnen, et al., 2020; Oktay et al., 2019; Singh et al., 2020; Minnen and Singh, 2020)). We have found this approach to yield reasonable results at higher rates, but at low rates, the ad-hoc nature of this approach leads to problematic behaviors of the transforms (RD performance plotted in fig. 3, illustration in fig. 7).

Agustsson and Theis (2020) discuss augmenting the transforms with a soft quantization function (and making appropriate modifications to the entropy model), which explicitly implements the curvature observed in fig. 4. The soft quantization function has a *temperature* parameter, interpolating between the identity function

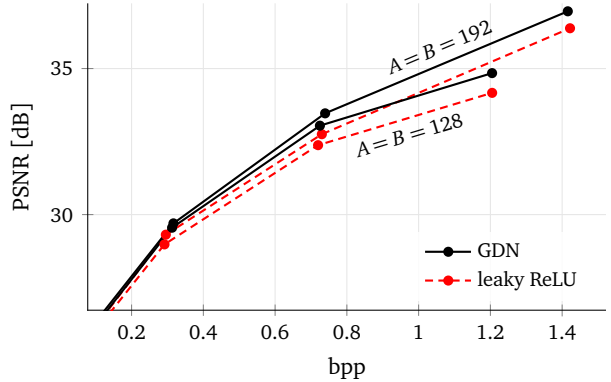


Figure 9: Rate-distortion performance of an image transform code with GDN vs. a typical pointwise non-linearity, reproduced from (Ballé, 2018). We compare networks with a different number of hidden units A, B . At low rates, the approximation capacity of all networks is sufficient, and performance converges. At high rates, the capacity of smaller networks saturates earlier; in this regime, performance differences between nonlinearities become measurable.

and hard quantization. By explicitly modeling this behavior, the technique relieves the ANN itself from implementing it (fig. 8), and represents a more principled approach to bridging the gap between quantization and additive uniform noise while retaining near-optimal performance at all rates (fig. 3). The temperature parameter allows explicitly trading off the bias of the proxy loss with the variance of the gradients. For simplicity, the experiments in this paper use the mode-centering approach.

3.2 Nonlinear transforms

ANNs are known as arbitrary function approximators, and as such we permitted ourselves to ignore their details in the examples above. However, it is crucial to take into account their limitations, some of which arise as a function of their architecture. This is particularly important for complex or high-dimensional source distributions, such as natural images. With higher complexity and rates (larger values of λ), the optimal transforms generally are more complex and require neural

networks with an increasing number of parameters.³

In general, neural networks are compositions of layers (parametric functions $\mathbb{R}^A \rightarrow \mathbb{R}^B$), wherein each layer typically consists of a linear transformation such as matrix multiplication or convolution, followed by the addition of a bias vector, followed in turn by a nonlinear function, which is typically applied separately on each vector dimension:

$$\mathbf{v} = g(\mathbf{r}), \text{ with } \mathbf{r} = \mathbf{W}\mathbf{u} + \mathbf{b}, \quad (15)$$

where $\mathbf{u} \in \mathbb{R}^A$ is the input vector to the layer, $\mathbf{v} \in \mathbb{R}^B$ are the layer’s outputs or *activations*, and $\mathbf{W} \in \mathbb{R}^{B \times A}$ and $\mathbf{b} \in \mathbb{R}^B$ are the layer’s parameters. For the NTC examples above, we used neural networks with 4 fully connected (i.e., non-convolutional) layers, the first three using the softplus nonlinearity ($g(x) = \log(1 + \exp(x))$ elementwise), while the last layer omits the nonlinearity in order not to constrain the range of the transform to positive values. The *approximation capacity*, i.e., the capability of the neural network to approximate increasingly complex functions, grows with the number of units per layer (A , B), as well as the depth of the network (the number of layers). Above, we chose $A = B = 100$ (except that we set $A = N$ for the first, and $B = M = N$ for the last layer in g_a ; analogous for g_s), which we found empirically to be large enough for all values of λ .

For practical sources such as images, video, or audio, imposing special structure in the transforms may have significant benefits in terms of computational complexity, training data efficiency, or both. Generally, nonlinear transform codes for this type of data use combinations of architectural constraints, most commonly *convolutionality* in g_a and g_s , as well as *downsampling* in g_a and *upsampling* in g_s , making the transforms share certain characteristics with multi-scale filterbanks, and leading to latent vectors with a tensor structure, consisting of one or more spatial/temporal dimensions, as well as one *channel* dimension (akin to subbands). A detailed example of such an architecture is described by Ballé, Laparra, and Simoncelli (2017).

³It could be argued that in the high-rate limit, the transforms should collapse to identity functions. However, we haven’t observed this effect for image compression models and practically interesting rate–distortion trade-offs, suggesting that this is only the case for extremely high rates.

It has been observed that spatially local normalization as a nonlinearity is beneficial in terms of the trade-off between number of units and RD performance in image compression. In particular, a computationally optimized version of generalized divisive normalization (GDN) (Ballé, Laparra, and Simoncelli, 2016a) as used in recent models is defined as

$$v_i = \frac{r_i}{\beta_i + \sum_j \gamma_{ij} |r_j|}, \quad (16)$$

where \mathbf{r} are the linear responses of the layer, \mathbf{v} represents the vector of normalized responses (the activations), and the vector β and matrix γ represent parameters of the transformation (both non-negative). The computation is typically replicated across spatial dimensions, as linear filtering is in convolutions, and i, j only index the channel dimension. Johnston et al. (2019) show that the originally more complex form of GDN can be simplified to resemble a weighted ℓ^1 -norm (plus a constant), as in eq. (16), with negligible RD performance loss, but minimizing computationally costly exponentiations. Since ANNs can be understood as universal function approximators, the benefit of a particular architectural constraint may only become evident when the network is at its approximation capacity. Ballé (2018) finds that this is the case at higher rates; i.e., for a constant network architecture, the superiority of GDN versus pointwise nonlinearities disappears at lower rates (fig. 9). Johnston et al. (2019) also discuss the trade-off between computational complexity and RD performance resulting from other architectural choices in further detail, such as the number of channels per layer or the number of decoder layers, and provide an algorithm to semi-automatically determine these hyperparameters.

4 Learned entropy models

In linear transform coding with a Gaussian source assumption, the probabilistic model P in eq. (9) is typically considered to be a distribution factorized over each latent dimension, since the KLT factorizes the source. However, as pointed out by Goyal (2001), this is not necessarily the case for real-world sources, and factorizing the source is not necessarily RD optimal, even

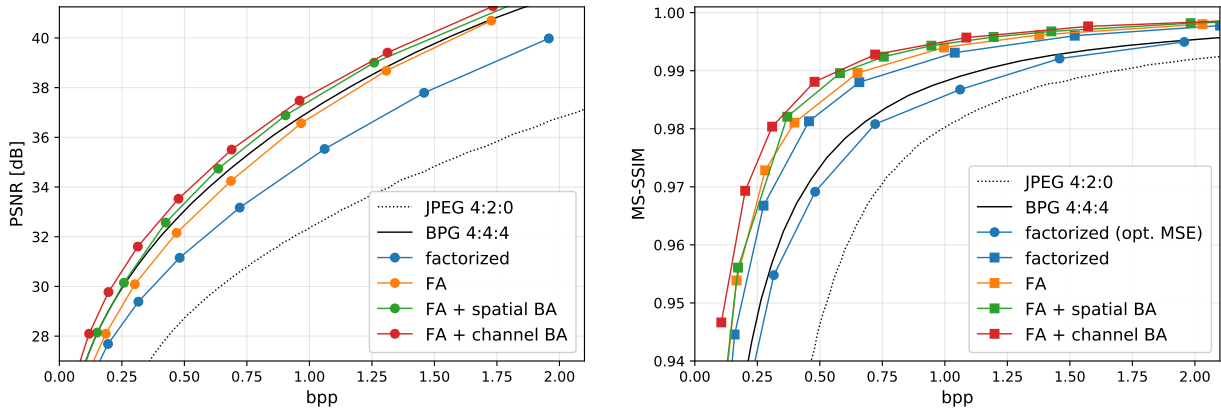


Figure 11: Image compression performance using nonlinear transform coding. We compare several learned image compression models to JPEG and BPG, which is a popular variant of HEVC, a relatively recent and popular commercial method. Conditional entropy models lead to significant improvements over factorized models. With sophisticated entropy modeling, learned image compression compares favorably to HEVC in terms of PSNR, which HEVC is optimized for. Regarding MS-SSIM, note that even the factorized model optimized for mean squared error (MSE) performs relatively closely to BPG, and when optimized for MS-SSIM, far outperforms it. We attribute this to the fact that regardless of the distortion metric, nonlinear transforms are better suited to model the source distribution, as illustrated in fig. 1, and MS-SSIM captures certain image features that are characteristic to the source.

zero-mean Gaussians, conditionally independent wrt. \hat{z} ; a non-zero mean model is introduced by Minnen, Ballé, and Toderici (2018). The entropy of \hat{z} is small enough to warrant the improved fit of $P(\hat{y} | \hat{z})$, effectively lowering the rate. Figure 11 compares the rate-distortion performance of several learned image compression models with JPEG (JPEG 1992) and BPG, a variant of HEVC (HEVC 2013), in terms of peak signal-to-noise ratio (PSNR) as well as MS-SSIM, a popular perceptual image quality metric (Z. Wang, Simoncelli, and Bovik, 2003). The introduction of FA into NTC leads to a significant improvement of RD performance with respect to both metrics.

Minnen, Ballé, and Toderici (2018) are among the first authors to discuss learned backward adaptation. They introduce a spatially autoregressive model, where y is processed one spatial location at a time, producing a distribution for each channel vector conditioned on previously decoded spatial locations. Combined with FA, the model produces further RD gains over the FA-only model (fig. 11), and outperforms BPG. However,

ANN-based compression methods benefit from computational parallelism, and the small scale of iterations makes it difficult to leverage GPU processors. Minnen and Singh (2020) introduce a model that instead iterates over channel slices, which is more amenable to hardware acceleration and, along with further modeling improvements, presents a significant improvement over traditional methods.

A problem frequently encountered with conditional entropy models is numerical determinism. To make image compression models practically relevant, they need to be implemented on a wide variety of hardware platforms. However, when probabilities are computed using floating-point arithmetic, numerical round-off errors can lead to catastrophic decoding failures due to the sensitivity of entropy coding with respect to discrepancies in the probability model between sender and receiver. The exact numerical round-off at each layer of an ANN depends on the hardware representation of floating point numbers, as well as the mode of parallelism, because round-off errors are not associa-

tive. This problem is typically handled in linear transform coders by using lookup tables to model probabilities (e.g., Marpe, Schwarz, and Wiegand, 2003). Ballé, Minnen, and Johnston (2018) provide a solution for ANN-based entropy modeling, where ANNs are trained using floating-point arithmetic, but use integer arithmetic when deployed. This enables reliable decoding on arbitrary hardware platforms for the above-mentioned class of entropy models.

5 RD parameterizing the transforms

The loss function in eq. (13) is optimized in expectation over the source distribution. The resulting transform thus jointly minimizes the rate and the expected distortion d between the source and the reconstruction, with the trade-off determined by λ . In many linear transform coders, the system is parameterized by the quantization step size. This is not the case for the previously discussed formulation. Rather, for each λ , a separate set of transforms and entropy models must be trained.

To substantially reduce the number of parameters of such a family of nonlinear transforms, the transforms and/or the entropy model can be made functions of λ , such that only one set of parameterized transforms and one entropy model is needed for a range of RD trade-offs. It is common to do this in ANNs by introducing additional computations between layers, such as affine transformations:

$$\mathbf{w} = h_f(\lambda) \odot \mathbf{v} + h_b(\lambda), \quad (18)$$

where \mathbf{v} are the outputs of a layer, \mathbf{w} are the inputs to the next layer, and \odot represents elementwise multiplication. h_f and h_b are parametric functions of λ that are either computed themselves via ANNs, or, since they are functions of a scalar, may be conveniently defined via first-order splines (i.e., piecewise linear functions). The parameters of these functions themselves are optimized for the RD objective (eq. (13)) as well. An alternative for transforms using GDN is to treat its parameters (β and γ) as functions of λ .

We carried out experiments with an NTC model with FA following Ballé, Minnen, Singh, et al. (2018), but

with 256 channels per layer. When implementing h_f and h_b with ANNs, we used two-layer networks with 128 hidden units for each scalar element produced by the functions. For the spline implementation, we used a first-order spline with 25 parameters. We found that the optimization of ANN-based parameterization is numerically more difficult than first-order splines (fig. 12, left panel). Furthermore, we removed the λ -parameterization of the entropy model and noted that it is not crucial to RD performance (right panel). Along with the practical requirement that h_s needs to be implemented with integer arithmetic for cross-platform stability, this suggests that making the entropy model explicitly dependent on λ may not be worth the complexity of implementation.

Figure 13 illustrates the RD performance of different parameterizations of the transforms g_a and g_s . As for the experiments with different nonlinearities, differences between the parameterizations emerge at high rates, since the network capacity saturates in that regime. We find that a scaling or affine transformation of the latent space alone, roughly equivalent to parameterizing the quantization step size and offset, are not sufficient to achieve an RD performance equivalent to the family of full, non-parameterized models. However, any layer-wise parameterization appears close enough. This is explainable by the fact that the RD family of optimal entropy-constrained scalar quantizers cannot in general be parameterized by a scaling of the quantization offset (a notable exception being the Laplace source discussed above). GDN reparameterization performs the best in an RD sense, but also requires slightly more model parameters compared to the other methods, since eq. (18) requires two length- B vectors, but γ is a $B \times B$ matrix.

6 Discussion

Due to the resurgence of ANNs and data-driven computing in recent years, the field of data compression has received an influx of new ideas. While transform coding as a concept has been around for decades (Ahmed and Rao, 1975), one could observe a recent convergence of it with the idea of autoencoders (Hinton and Salakhutdinov, 2006). Autoencoders, likewise, have been dis-

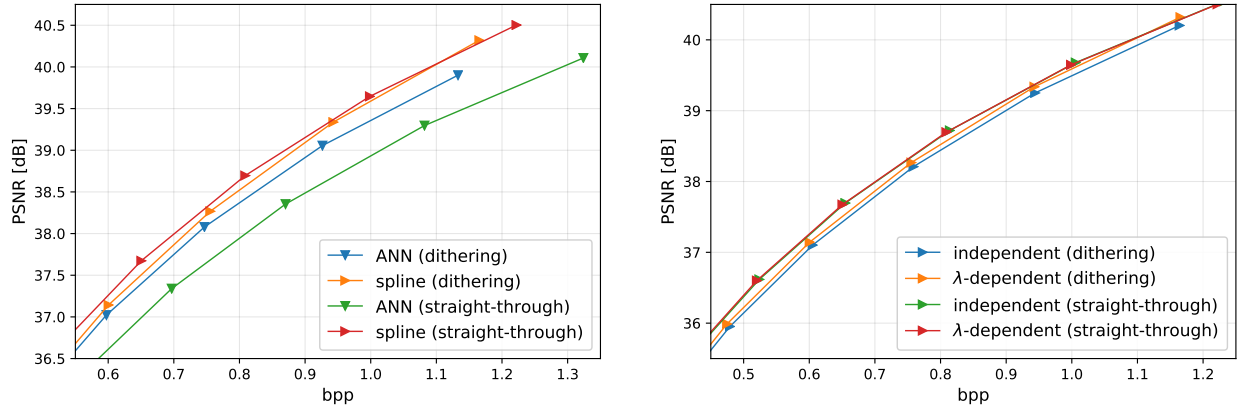


Figure 12: Performance comparisons of different λ -parameterization techniques for models of the same architecture, and using eq. (18) for each layer of the transforms, as well as for each layer of a forward-adaptive entropy model. As in fig. 9, differences between models become more evident at high rates. Both comparisons yield consistent results regardless of whether the models are optimized using the dithering proxy or the straight-through proxy. Left: comparison of models implementing h_f and h_b using ANNs vs. using first-order splines. We find that the performance of ANNs is consistently worse than that of splines, despite a larger number of parameters, suggesting that optimization of ANNs in this context may be numerically more difficult than that of spline parameters. Right: comparison of models using either a λ -parameterized entropy model, or a forward-adaptive entropy model independent of λ . We find that the benefit of parameterization in terms of RD performance is rather small, especially considering that it is not trivial to parameterize an ANN using integer arithmetic, as is necessary in the entropy model for reliable cross-platform decoding.

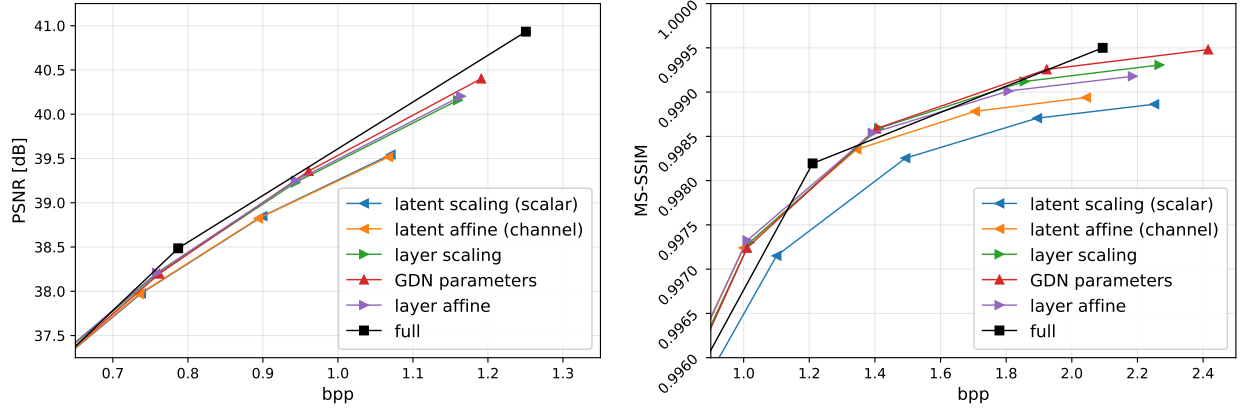


Figure 13: Performance comparison of different λ -parameterization techniques using first-order splines in eq. (18), and parameterizing only the transforms, not the entropy model. All models have the same architecture and were optimized using the dithering proxy either for MSE (left panel) or MS-SSIM (right panel). As in fig. 9, differences between models become more evident at high rates. Optimization using the straight-through proxy gives consistent results (not shown). *Full*: RD performance of separate models for each λ ; *latent scaling*: only the output of the g_a and the input to g_s are scaled with a single scalar each (h_b is zero); *latent affine*: each output channel of g_a and each input channel of g_s are subjected to a scalar affine transformation, as in eq. (18); *layer affine*: each channel of each layer of g_a and g_s is subjected to a scalar affine transformation; *layer scaling*: ditto, except that h_b is zero; *GDN parameters*: rather than adding a scaling between layers, the parameters of each instance of GDN in the transforms (β and γ) are represented as first-order splines dependent on λ . We note that a simple affine transformation of the latent space, corresponding to varying the quantization interval, is not sufficient to maintain comparable performance with the full model. Scaling the activations of each layer appears sufficient, while reparameterizing GDN as a function of λ yields slightly better performance.

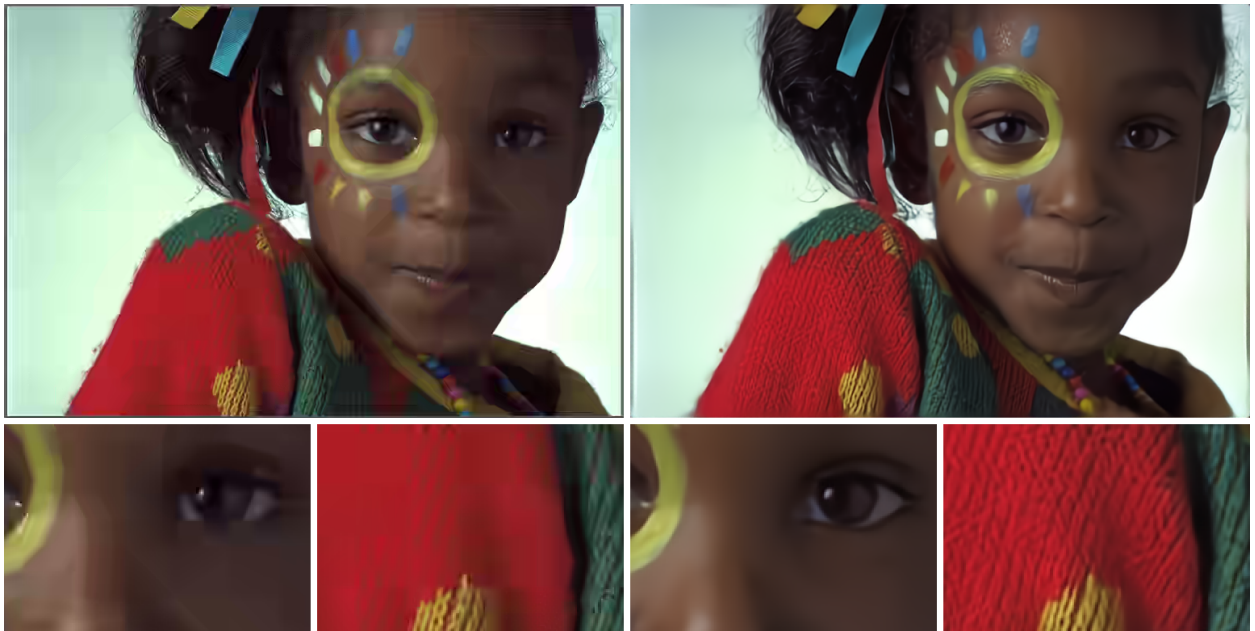


Figure 14: Reconstructions of kodim15 (Kodak, 1993) compressed by BPG (left, 0.0738 bpp) and by a learned NTC model (Minnen and Singh, 2020) optimized for MS-SSIM (right, 0.0713 bpp). The combination of NTC and an MS-SSIM loss function, which is designed to model texture masking effects in the human visual system, leads to significantly better texture retention in the sweater and fewer geometric distortions on the person’s face.

cussed for decades, but largely in a separate community. One notable step towards this convergence was the fusion of variational Bayesian methods with autoencoders, which introduced a probabilistic interpretation, making the connection to information-theoretic quantities such as entropy (Kingma and Welling, 2014; Rezende, Mohamed, and Wierstra, 2014); another was the use of a dithering-based loss for optimization of nonlinear transform codes (Ballé, Laparra, and Simoncelli, 2016b).

As is often the case in lossy compression, the field of nonlinear transform coding has been driven forward by the need to compress digital images. Early image compression models using ANNs include the work of Toderici, Vincent, et al. (2017) and Covell et al. (2017), who do not use entropy modeling; Rippel and Bourdev (2017), who use a context-based adaptive entropy coder that isn't jointly optimized with the transforms; and Ballé, Laparra, and Simoncelli (2017) and Theis et al. (2017), who jointly optimize the transforms with continuous entropy models, the latter with a different formulation than what we use in this paper. Agustsson, Mentzer, et al. (2017) notably combine an autoencoder with VQ in the latent space over small blocks of coefficients, utilizing a soft quantization proxy. More recent work using soft notions of quantization includes the work of Alexandre et al. (2019) and Agustsson and Theis (2020).

Beyond the use of convolutional filtering, up- or downsampling, and special nonlinearities (Ballé, Laparra, and Simoncelli, 2017) as discussed earlier, many authors exploit properties of the image distribution by way of introducing special structure into the transforms, such as multi-scale architectures (Rippel and Bourdev, 2017; Nakanishi et al., 2018; C. Cai et al., 2018); non-local, or “attention”-based network architectures (H. Liu et al., 2019; T. Chen et al., 2019); or iteration built into the transforms (J. Cai and L. Zhang, 2018; Mali et al., 2018). Recently, the topic of extending nonlinear transform codes to video signals has received much attention, and the space of possible network architectures suitable for this application has been explored, including spatiotemporal convolutions, optical flow networks, as well as multi-scale linear filtering (Wu, Singhal, and Krahenbuhl, 2018; Jun Han et al., 2018; Lu, Ouyang, et al., 2019; Z. Chen et al.,

2019; Rippel, Nair, et al., 2019; Habibian et al., 2019; Djelouah et al., 2019; Lombardo et al., 2019; Golinski et al., 2020; R. Yang et al., 2020; Lu, X. Zhang, et al., 2020; Agustsson, Minnen, et al., 2020). Ballé, Minnen, and Johnston (2018) develop integer architectures for learned entropy models, in order to guarantee reliable decoding on arbitrary hardware platforms, and Johnston et al. (2019) discuss selecting architecture parameters, such as the number of layers, or number of channels per layer, while taking into account the RD performance.

Notable work in the space of learned entropy models includes Minnen, Toderici, et al. (2018), which use block-based forward adaptation, and several other concurrent publications performing learned backward adaptation (Minnen, Ballé, and Toderici, 2018; Jooyoung Lee, Cho, and Beack, 2018; Mentzer, Agustsson, Tschannen, Timofte, and Van Gool, 2018). More recent work on learned backward adaptation includes the papers by M. Li, K. Ma, et al. (2020) and Guo et al. (2020).

The first work exploring the rate-distortion trade-off of a nonlinear transform coder with a single model parameterized for λ is due to Dumas, Roumy, and Guillemot (2018), who explore varying the quantization step size, as in linear TC (corresponding most closely to “latent affine” in fig. 13). Guarda, Rodrigues, and Pereira (2020) use the same method for coding point-cloud geometries. Layer-wise parameterization as in eq. (18), while originally introduced in the context of image stylization (Dumoulin, Shlens, and Kudlur, 2017), was introduced for image compression by Choi, El-Khamy, and Jungwon Lee (2019). It was generalized by Dosovitskiy and Djolonga (2019) for a range of other tasks including compression. To our knowledge, we provide the first direct comparison of different approaches in this paper, and also introduce a new one (GDN parameterization).

While many authors have explored ANN-based compression in the context of existing, commercially viable image and video compression methods (Jiang et al., 2017; J. Li et al., 2018; Jia et al., 2019; D. Liu, H. Ma, et al., 2018; Hu et al., 2019), other authors begin with nonlinear transforms, and explore incorporating concepts traditionally used in linear TC, such as energy compaction (Cheng, Sun, et al., 2019), wavelets (Akyazi and Ebrahimi, 2019; C. Yang, Zhao, and S.

Wang, 2019), or trellis coded quantization (D. Liu, Y. Li, et al., 2020). Lossless image compression based on learned entropy models has been explored by, e.g. Mentzer, Agustsson, Tschannen, Timofte, and Van Gool (2018) and Mentzer, Agustsson, Tschannen, Timofte, and Gool (2019). Still others explore the intersection between learned image compression and other vision tasks such as content and semantic analysis (M. Li, Zuo, et al., 2018; Campos et al., 2019; Akbari, Liang, and Jingning Han, 2019; Luo et al., 2018), inpainting (Baig, Koltun, and Torresani, 2017), super-resolution (Cao, Wu, and Krähenbühl, 2020), quality enhancement (Jooyoung Lee, Cho, and Kim, 2019), or encryption (Duan, J. Liu, and E. Zhang, 2019).

Another topic of active research is the question of more “perceptual” image compression. In contrast to traditional image compression systems, NTC models can be directly optimized for any differentiable loss function modeling subjective image quality. An illustration of this is provided in fig. 14. For further notes regarding optimization of NTC models for squared error vs. MS-SSIM, refer to Ballé, Minnen, Singh, et al. (2018). Ding et al. (2020) provide a more in-depth discussion, with an even larger set of different perceptual distortion metrics. Interestingly, L.-H. Chen et al. (2019) provide a method to optimize NTC models for non-differentiable perceptual metrics. Valenzise et al. (2018), Cheng, Akyazi, et al. (2019), and Ascenso et al. (2020) study the perceived image quality of learned image compression models optimized for metrics such as squared error and MS-SSIM with the help of human rating experiments. Other authors have explored replacing the fixed distortion metric with ANN-based losses that have shown visually convincing results in image generation tasks, most notably generative adversarial networks (GANs) (Santurkar, Budden, and Shavit, 2018; Agustsson, Tschannen, et al., 2019; Tschannen, Agustsson, and Lucic, 2018; Kudo et al., 2019; Mentzer, Toderici, et al., 2020). Blau and Michaeli (2019) formulate theoretical limits for the three-way trade-off between the rate, the reconstruction quality of an image compression method, as well as divergence measures between the source distribution and the marginal distribution of image reconstructions, the latter of which are related to GAN objectives.

While image compression dominates the literature on

NTC, other applications have emerged as well, such as compression of point clouds (Quach, Valenzise, and Dufaux, 2019; Guarda, Rodrigues, and Pereira, 2020), volumetric data (Tang et al., 2020), ANN features for tasks like large-scale image retrieval (Singh et al., 2020), and compression of ANN parameters themselves (Oktay et al., 2019). Further reviews of the current state of the literature, specifically with respect to image and video compression, are given by S. Ma et al. (2019) and D. Liu, Y. Li, et al. (2020).

Being based on artificial neural networks and stochastic optimization, nonlinear transform coding enables much faster development cycles than traditional compression methods, and has witnessed remarkable performance gains within only a few years. With the rapidly increasing availability of parallelized computation, we believe it will fundamentally change the landscape of practical data compression.

Acknowledgements

The authors would like to thank Lucas Theis and Aaron Wagner for helpful discussions.

References

- Agustsson, Eirikur, Fabian Mentzer, et al. (2017). “Soft-to-Hard Vector Quantization for End-to-End Learning Compressible Representations”. In: *Advances in Neural Information Processing Systems* 30, pp. 1141–1151.
- Agustsson, Eirikur, David Minnen, et al. (2020). “Scale-Space Flow for End-to-End Optimized Video Compression”. In: *Proc. of the IEEE/CVF Conference on Computer Vision and Pattern Recognition*, pp. 8503–8512.
- Agustsson, Eirikur and Lucas Theis (2020). “Universally Quantized Neural Compression”. In: *arXiv e-prints*. eprint: 2006.09952.
- Agustsson, Eirikur, Michael Tschannen, et al. (2019). “Generative adversarial networks for extreme learned image compression”. In: *Proc. of the IEEE International Conference on Computer Vision*, pp. 221–231.
- Ahmed, N. and K. R. Rao (1975). *Orthogonal Transforms for Digital Signal Processing*. Springer. ISBN: 978-3-642-45452-3.

- Akbari, Mohammad, Jie Liang, and Jingning Han (2019). “DSSLIC: Deep semantic segmentation-based layered image compression”. In: *ICASSP 2019-2019 IEEE International Conference on Acoustics, Speech and Signal Processing (ICASSP)*. IEEE, pp. 2042–2046.
- Akyazi, Pinar and Touradj Ebrahimi (2019). “Learning-based image compression using convolutional autoencoder and wavelet decomposition”. In: *IEEE Conference on Computer Vision and Pattern Recognition Workshops*. CONF.
- Alemi, Alexander A. et al. (2018). “Fixing a Broken ELBO”. In: *Proc. of the 35th Int. Conf. on Machine Learning*. Vol. 80. Proc. of Machine Learning Research. URL: <https://openreview.net/forum?id=SyEdzh-uWr>.
- Alexandre, David et al. (2019). “Learned image compression with soft bit-based rate-distortion optimization”. In: *2019 IEEE International Conference on Image Processing (ICIP)*. IEEE, pp. 1715–1719.
- Ascenso, Joao et al. (2020). “Learning-based image coding: early solutions reviewing and subjective quality evaluation”. In: *Optics, Photonics and Digital Technologies for Imaging Applications VI*. Vol. 11353. International Society for Optics and Photonics, 113530S.
- Baig, Mohammad Haris, Vladlen Koltun, and Lorenzo Torresani (2017). “Learning to inpaint for image compression”. In: *Advances in Neural Information Processing Systems*, pp. 1246–1255.
- Ballé, Johannes (2018). “Efficient Nonlinear Transforms for Lossy Image Compression”. In: *Picture Coding Symposium (PCS), 2018*. DOI: 10.1109/PCS.2018.8456272.
- Ballé, Johannes, Valero Laparra, and Eero P. Simoncelli (2016a). “Density Modeling of Images Using a Generalized Normalization Transformation”. In: *arXiv e-prints*. Presented at the 4th Int. Conf. on Learning Representations. arXiv: 1511.06281.
- (2016b). “End-to-end optimization of nonlinear transform codes for perceptual quality”. In: *Picture Coding Symposium (PCS), 2016*. DOI: 10.1109/PCS.2016.7906310.
- (2017). “End-to-end Optimized Image Compression”. In: *Proc. of 5th Int. Conf. on Learning Representations*. URL: <https://openreview.net/forum?id=rJxdQ3jeg>.
- Ballé, Johannes, David Minnen, and Nick Johnston (2018). “Integer Networks for Data Compression with Latent-Variable Models”. In: *Proc. of Int. Conf. on Learned Representations*. URL: <https://openreview.net/forum?id=S1zz2i0cY7>.
- Ballé, Johannes, David Minnen, Saurabh Singh, et al. (2018). “Variational image compression with a scale hyperprior”. In: *Proc. of 6th Int. Conf. on Learning Representations*. URL: <https://openreview.net/forum?id=rkcQFMZRB>.
- Bennett, W. R. (1948). “Spectra of quantized signals”. In: *Bell System Technical Journal* 27, pp. 446–472.
- Berger, T. (1972). “Optimum quantizers and permutation codes”. In: *IEEE Transactions on Information Theory* 18, pp. 759–765.
- Blau, Yochai and Tomer Michaeli (2019). “Rethinking Lossy Compression: The Rate-Distortion-Perception Tradeoff”. In: *International Conference on Machine Learning*, pp. 675–685.
- Bottou, Leon and Yoshua Bengio (1995). “Convergence properties of the k-means algorithms”. In: *Advances in neural information processing systems*, pp. 585–592.
- Cai, Chunlei et al. (2018). “Efficient variable rate image compression with multi-scale decomposition network”. In: *IEEE Transactions on Circuits and Systems for Video Technology* 29.12, pp. 3687–3700.
- Cai, Jianrui and Lei Zhang (2018). “Deep image compression with iterative non-uniform quantization”. In: *2018 25th IEEE International Conference on Image Processing (ICIP)*. IEEE, pp. 451–455.
- Campos, Joaquim et al. (2019). “Content Adaptive Optimization for Neural Image Compression”. In: *Proc. of the IEEE Conference on Computer Vision and Pattern Recognition Workshops*.
- Cao, Sheng, Chao-Yuan Wu, and Philipp Krähenbühl (2020). “Lossless Image Compression through Super-Resolution”. In: *arXiv preprint arXiv:2004.02872*.
- Chen, Li-Heng et al. (2019). “ProxIQ: A Proxy Approach to Perceptual Optimization of Learned Image Compression”. In: *arXiv preprint arXiv:1910.08845*.
- Chen, Tong et al. (2019). “Neural image compression via non-local attention optimization and improved context modeling”. In: *arXiv preprint arXiv:1910.06244*.
- Chen, Zhibo et al. (2019). “Learning for video compression”. In: *IEEE Transactions on Circuits and Systems for Video Technology* 30.2, pp. 566–576.
- Cheng, Zhengxue, Pinar Akyazi, et al. (2019). “Perceptual quality study on deep learning based image compression”. In: *2019 IEEE International Conference on Image Processing (ICIP)*. IEEE, pp. 719–723.
- Cheng, Zhengxue, Heming Sun, et al. (2019). “Energy compaction-based image compression using convolutional autoencoder”. In: *IEEE Transactions on Multimedia* 22.4, pp. 860–873.
- Choi, Yoojin, Mostafa El-Khamy, and Jungwon Lee (2019). “Variable rate deep image compression with a conditional autoencoder”. In: *Proc. of the IEEE International Conference on Computer Vision*, pp. 3146–3154.
- Chou, Philip A, Tom Lookabaugh, and Robert M Gray (1989). “Entropy-constrained vector quantization”. In: *IEEE Trans-*

- actions on Acoustics, Speech, and Signal Processing 37.1, pp. 31–42.
- Covell, Michele et al. (2017). “Target-quality image compression with recurrent, convolutional neural networks”. In: *arXiv preprint arXiv:1705.06687*.
- Cover, Thomas M. and Joy A. Thomas (2006). *Elements of Information Theory*. 2nd ed. Wiley.
- Ding, Keyan et al. (2020). “Comparison of Image Quality Models for Optimization of Image Processing Systems”. In: *arXiv*, arXiv-2005.
- Djelouah, Abdelaziz et al. (2019). “Neural inter-frame compression for video coding”. In: *Proc. of the IEEE International Conference on Computer Vision*, pp. 6421–6429.
- Dosovitskiy, Alexey and Josip Djolonga (2019). “You Only Train Once: Loss-Conditional Training of Deep Networks”. In: *International Conference on Learning Representations*.
- Duan, Xintao, Jingjing Liu, and En Zhang (2019). “Efficient image encryption and compression based on a VAE generative model”. In: *Journal of Real-Time Image Processing* 16.3, pp. 765–773.
- Dumas, Thierry, Aline Roumy, and Christine Guillemot (2018). “Autoencoder based image compression: can the learning be quantization independent?” In: *2018 IEEE International Conference on Acoustics, Speech and Signal Processing (ICASSP)*. IEEE, pp. 1188–1192.
- Dumoulin, Vincent, Jonathon Shlens, and Manjunath Kudlur (2017). “A Learned Representation for Artistic Style”. In: *Proc. of Int. Conf. on Learned Representations*. URL: <https://openreview.net/forum?id=BJ0-BuT1g>.
- Favardin, N. and J. W. Modestino (1984). “Optimum quantizer performance for a class of non-Gaussian memoryless sources”. In: *IEEE Transactions on Information Theory* 30, pp. 485–497.
- Gersho, A. (1979). “Asymptotically optimal block quantization”. In: *IEEE Transactions on Information Theory* 25.4, pp. 373–380.
- Gersho, Allen and Robert M. Gray (1992). *Vector Quantization and Signal Compression*. Kluwer. ISBN: 978-0-7923-9181-4.
- Golinski, Adam et al. (2020). “Feedback Recurrent Autoencoder for Video Compression”. In: *arXiv preprint arXiv:2004.04342*.
- Goyal, Vivek K. (2001). “Theoretical Foundations of Transform Coding”. In: *IEEE Signal Processing Magazine* 18.5. DOI: 10.1109/79.952802.
- Guarda, André FR, Nuno MM Rodrigues, and Fernando Pereira (2020). “Deep Learning-Based Point Cloud Geometry Coding: RD Control Through Implicit and Explicit Quantization”. In: *2020 IEEE International Conference on Multimedia & Expo Workshops (ICMEW)*. IEEE, pp. 1–6.
- Guo, Zongyu et al. (2020). “3-D Context Entropy Model for Improved Practical Image Compression”. In: *Proc. of the IEEE/CVF Conf. on Computer Vision and Pattern Recognition Workshops*, pp. 116–117.
- Habibian, Amirhossein et al. (2019). “Video compression with rate-distortion autoencoders”. In: *Proc. of the IEEE International Conference on Computer Vision*, pp. 7033–7042.
- Han, Jun et al. (2018). “Deep probabilistic video compression”. In: *arXiv preprint arXiv:1810.02845*.
- Higgins, Irina et al. (2017). “ β -VAE: Learning Basic Visual Concepts with a Constrained Variational Framework”. In: *Proc. of 5th Int. Conf. on Learning Representations*. URL: <https://openreview.net/forum?id=Sy2fzU9gl>.
- Hinton, Geoffrey E. and R. R. Salakhutdinov (2006). “Reducing the Dimensionality of Data with Neural Networks”. In: *Science* 313.5786. DOI: 10.1126/science.1127647.
- Hu, Yueyu et al. (2019). “Progressive spatial recurrent neural network for intra prediction”. In: *IEEE Transactions on Multimedia* 21.12, pp. 3024–3037.
- HEVC (2013). *ITU-R Rec. H.265 & ISO/IEC 23008-2: High Efficiency Video Coding*.
- JPEG (1992). *ITU-R Rec. T.81 & ISO/IEC 10918-1: Digital compression and coding of continuous-tone still images*.
- Jia, Chuanmin et al. (2019). “Content-aware convolutional neural network for in-loop filtering in high efficiency video coding”. In: *IEEE Transactions on Image Processing* 28.7, pp. 3343–3356.
- Jiang, Feng et al. (2017). “An end-to-end compression framework based on convolutional neural networks”. In: *IEEE Transactions on Circuits and Systems for Video Technology* 28.10, pp. 3007–3018.
- Johnston, Nick et al. (2019). “Computationally Efficient Neural Image Compression”. In: *arXiv e-prints*. eprint: 1912.08771.
- Kingma, Diederik P. and Max Welling (2014). “Auto-Encoding Variational Bayes”. In: *arXiv e-prints*. Presented at the 2nd Int. Conf. on Learning Representations. arXiv: 1312.6114.
- Kodak, Eastman (1993). *Kodak Lossless True Color Image Suite (PhotoCD PCD0992)*. URL: <http://r0k.us/graphics/kodak/>.
- Kudo, Shinobu et al. (2019). “GAN-based Image Compression Using Mutual Information Maximizing Regularization”. In: *2019 Picture Coding Symposium (PCS)*. IEEE, pp. 1–5.
- Lee, Jooyoung, Seunghyun Cho, and Seung-Kwon Beack (2018). “Context-adaptive Entropy Model for End-to-end Optimized Image Compression”. In: *International Conference on Learning Representations*.
- Lee, Jooyoung, Seunghyun Cho, and Munchurl Kim (2019). “A hybrid architecture of jointly learning image compres-

- sion and quality enhancement with improved entropy minimization". In: *arXiv preprint arXiv:1912.12817*.
- Leshno, Moshe et al. (1993). "Multilayer Feedforward Networks With a Nonpolynomial Activation Function Can Approximate Any Function". In: *Neural Networks* 6.6. DOI: 10.1016/S0893-6080(05)80131-5.
- Li, Jiahao et al. (2018). "Fully connected network-based intra prediction for image coding". In: *IEEE Transactions on Image Processing* 27.7, pp. 3236–3247.
- Li, Mu, Kede Ma, et al. (2020). "Efficient and Effective Context-Based Convolutional Entropy Modeling for Image Compression". In: *IEEE Transactions on Image Processing* 29, pp. 5900–5911.
- Li, Mu, Wangmeng Zuo, et al. (2018). "Learning convolutional networks for content-weighted image compression". In: *Proc. of the IEEE Conference on Computer Vision and Pattern Recognition*, pp. 3214–3223.
- Linde, Y., A. Buzo, and R. M. Gray (1980). "An algorithm for vector quantizer design". In: *IEEE Transactions on Communications* 28, pp. 84–95.
- Liu, Dong, Yue Li, et al. (2020). "Deep learning-based video coding: A review and a case study". In: *ACM Computing Surveys (CSUR)* 53.1, pp. 1–35.
- Liu, Dong, Haichuan Ma, et al. (2018). "CNN-based DCT-like transform for image compression". In: *International Conference on Multimedia Modeling*. Springer, pp. 61–72.
- Liu, Haojie et al. (2019). "Non-local attention optimized deep image compression". In: *arXiv preprint arXiv:1904.09757*.
- Lloyd, S. P. (1982). "Least squares quantization in PCM". In: *IEEE Transactions on Information Theory* 28. (Previously an unpublished Bell Lab Tech. Note, 1957.), pp. 129–136.
- Lombardo, Salvator et al. (2019). "Deep generative video compression". In: *Advances in Neural Information Processing Systems*, pp. 9287–9298.
- Lu, Guo, Wanli Ouyang, et al. (2019). "Dvc: An end-to-end deep video compression framework". In: *Proc. of the IEEE Conference on Computer Vision and Pattern Recognition*, pp. 11006–11015.
- Lu, Guo, Xiaoyun Zhang, et al. (2020). "An End-to-End Learning Framework for Video Compression". In: *IEEE Transactions on Pattern Analysis and Machine Intelligence*.
- Luo, Sihui et al. (2018). "DeepSIC: Deep semantic image compression". In: *International Conference on Neural Information Processing*. Springer, pp. 96–106.
- Ma, Siwei et al. (2019). "Image and video compression with neural networks: A review". In: *IEEE Transactions on Circuits and Systems for Video Technology*.
- MacQueen, James et al. (1967). "Some methods for classification and analysis of multivariate observations". In: *Proc. of the fifth Berkeley symposium on mathematical statistics and probability*. Vol. 1. 14. Oakland, CA, USA, pp. 281–297.
- Mali, Ankur et al. (2018). "Learned iterative decoding for lossy image compression systems". In: *arXiv preprint arXiv:1803.05863* 1.
- Marpe, Detlev, Heiko Schwarz, and Thomas Wiegand (2003). "Context-Based Adaptive Binary Arithmetic Coding in the H.264/AVC Video Compression Standard". In: *IEEE Transactions on Circuits and Systems for Video Technology* 13.7. DOI: 10.1109/TCSVT.2003.815173.
- Max, J. (1960). "Quantizing for minimum distortion". In: *IRE Transactions on Information Theory* 6, pp. 7–12.
- Mentzer, Fabian, Eirikur Agustsson, Michael Tschannen, Radu Timofte, and Luc Van Gool (2019). "Practical full resolution learned lossless image compression". In: *Proc. of the IEEE Conference on Computer Vision and Pattern Recognition*, pp. 10629–10638.
- Mentzer, Fabian, Eirikur Agustsson, Michael Tschannen, Radu Timofte, and Luc Van Gool (2018). "Conditional probability models for deep image compression". In: *Proc. of the IEEE Conference on Computer Vision and Pattern Recognition*, pp. 4394–4402.
- Mentzer, Fabian, George Toderici, et al. (2020). "High-Fidelity Generative Image Compression". In: *arXiv preprint arXiv:2006.09965*.
- Minnen, David, Johannes Ballé, and George Toderici (2018). "Joint Autoregressive and Hierarchical Priors for Learned Image Compression". In: *Advances in Neural Information Processing Systems* 31, pp. 10771–10780.
- Minnen, David and Saurabh Singh (2020). "Channel-Wise Autoregressive Entropy Models for Learned Image Compression". In: *Proc. of IEEE Int. Conf. on Image Processing ICIP*. submitted.
- Minnen, David, George Toderici, et al. (2018). "Image-dependent local entropy models for learned image compression". In: *2018 25th IEEE International Conference on Image Processing (ICIP)*. IEEE, pp. 430–434.
- Nakanishi, Ken M et al. (2018). "Neural multi-scale image compression". In: *Asian Conference on Computer Vision*. Springer, pp. 718–732.
- Oktay, Deniz et al. (2019). "Scalable Model Compression by Entropy Penalized Reparameterization". In: *International Conference on Learning Representations*.
- Quach, Maurice, Giuseppe Valenzise, and Frederic Dufaux (2019). "Learning convolutional transforms for lossy point cloud geometry compression". In: *2019 IEEE International Conference on Image Processing (ICIP)*. IEEE, pp. 4320–4324.
- Rezende, Danilo J., Shakir Mohamed, and Daan Wierstra (2014). "Stochastic Backpropagation and Approximative

- Inference in Deep Generative Models”. In: *Proc. of Machine Learning Research*. Vol. 32. 2, pp. 1278–1286.
- Rippel, Oren and Lubomir Bourdev (2017). “Real-Time Adaptive Image Compression”. In: *Proc. of Machine Learning Research*. Vol. 70, pp. 2922–2930.
- Rippel, Oren, Sanjay Nair, et al. (2019). “Learned video compression”. In: *Proc. of the IEEE International Conference on Computer Vision*, pp. 3454–3463.
- Santurkar, Shibani, David Budden, and Nir Shavit (2018). “Generative compression”. In: *2018 Picture Coding Symposium (PCS)*. IEEE, pp. 258–262.
- Schuchman, Leonard (1964). “Dither Signals and Their Effect on Quantization Noise”. In: *IEEE Transactions on Communication Technology* 12.4. DOI: 10.1109/TCOM.1964.1088973.
- Singh, Saurabh et al. (2020). “End-to-end Learning of Compressible Features”. In: *Proc. of IEEE Int. Conf. on Image Processing ICIP*.
- Sullivan, Gary J. (1996). “Efficient scalar quantization of exponential and Laplacian random variables”. In: *IEEE Transactions on Information Theory* 42.5. DOI: 10.1109/18.532878.
- Tang, Danhang et al. (2020). “Deep Implicit Volume Compression”. In: *Proc. of the IEEE/CVF Conference on Computer Vision and Pattern Recognition*, pp. 1293–1303.
- Theis, Lucas et al. (2017). “Lossy Image Compression with Compressive Autoencoders”. In: *Proc. of 5th Int. Conf. on Learning Representations*. URL: <https://openreview.net/forum?id=rJiNwv9gg>.
- Toderici, George, Sean M. O’Malley, et al. (2016). “Variable Rate Image Compression with Recurrent Neural Networks”. In: *arXiv e-prints*. Presented at the 4th Int. Conf. on Learning Representations. arXiv: 1511.06085.
- Toderici, George, Damien Vincent, et al. (2017). “Full Resolution Image Compression with Recurrent Neural Networks”. In: *2017 IEEE Conf. on Computer Vision and Pattern Recognition (CVPR)*. DOI: 10.1109/CVPR.2017.577. arXiv: 1608.05148.
- Tschannen, Michael, Eirikur Agustsson, and Mario Lucic (2018). “Deep generative models for distribution-preserving lossy compression”. In: *Advances in Neural Information Processing Systems*, pp. 5929–5940.
- Valenzise, Giuseppe et al. (2018). “Quality assessment of deep-learning-based image compression”. In: *2018 IEEE 20th International Workshop on Multimedia Signal Processing (MMSP)*. IEEE, pp. 1–6.
- Wang, Zhou, Eero P. Simoncelli, and Alan Conrad Bovik (2003). “Multi-Scale Structural Similarity for Image Quality Assessment”. In: *Conf. Rec. of the 37th Asilomar Conf. on Signals, Systems and Computers*. DOI: 10.1109/ACSSC.2003.1292216.
- Wu, Chao-Yuan, Nayan Singhal, and Philipp Krahenbuhl (2018). “Video compression through image interpolation”. In: *Proc. of the European Conference on Computer Vision (ECCV)*, pp. 416–431.
- Yang, Chuxi, Yan Zhao, and Shigang Wang (2019). “Deep image compression in the wavelet transform domain based on high frequency sub-band prediction”. In: *IEEE Access* 7, pp. 52484–52497.
- Yang, Ren et al. (2020). “Learning for Video Compression with Recurrent Auto-Encoder and Recurrent Probability Model”. In: *arXiv preprint arXiv:2006.13560*.